Sub 100 nm proton beam micromachining: theoretical calculations on resolution limits

J.A. van Kan [*], T.C. Sum, T. Osipowicz, F. Watt

Research Centre for Nuclear Microscopy, Department of Physics, National University of Singapore, Lower Kent Ridge Road, Singapore 119260, Singapore

Abstract

Proton beam micromachining is a novel direct-write process for the production of three-dimensional (3D) microstructures. A focused beam of MeV protons is scanned in a pre-determined pattern over a suitable resist material (e.g. PMMA or SU-8) and the latent image formed is subsequently developed chemically. In this paper calculations on theoretical resolution limits of proton beam micromachined three-dimensional microstructures are presented. Neglecting the finite beam size, a Monte Carlo ion transport code was used in combination with a theoretical model describing the delta-ray (δ-ray) energy deposition to determine the lateral energy deposition distribution in PMMA resist material. The energy deposition distribution of ion induced secondary electrons (δ-rays) has been parameterized using analytical models. It is assumed that the attainable resolution is limited by a convolution of the spread of the ion beam and energy deposition of the δ-rays. © 2000 Elsevier Science B.V. All rights reserved.

1. Introduction

Proton beam micromachining using MeV protons is a technique that is able to produce three-dimensional (3D) microstructures in resist material. Recently, proton beam micromachining has demonstrated great potential for the production of intricate 3D microstructures in positive resists such as PMMA as well as in negative resists such as SU-8 [1], with feature dimensions down to 150 nm [2–5]. The smallest feature size attainable is determined by the lateral dose distribution of the ion beam, which varies as a function of proton penetration depth in the resist. It is well-known that the proton deviates from the ideal straight path due to multiple small angle coulomb scattering (neglecting Rutherford collisions). In addition however, the lateral dose distribution is also influenced by the energy deposition of secondary electrons (δ-rays). As compared to δ-ray generation in the case of electron beam lithography, the δ-rays generated by MeV protons play a reduced role in the lateral dose distribution because of the high

---
[*] Corresponding author. Tel.: +65-874-2624; fax: +65-777-6126.

E-mail address: phyjavk@nus.edu.sg (J.A. van Kan).

mass of the proton compared to the electron and the correspondingly smaller energy transfer.

Examples of microstructures produced using proton beam micromachining in positive resist as well as in negative resist will be used to demonstrate the effects of the lateral dose distribution with depth. Calculations are presented to establish the role of δ-rays in the energy deposition for proton beam micromachining using proton energies of 2.0 and 3.5 MeV. Finally we present the results of theoretical calculations to indicate the optimum experimental conditions to produce high aspect ratio, sub 100 nm microstructures using proton beam micromachining. At this preliminary stage we are considering the effects of a point-like parallel beam only, and have not included the practical effects of beam divergence and finite beam size due to beam focusing.

2. Procedure

There are two major factors which influence the capabilities of producing sharp and well-defined microstructures with sub-micrometer details in the lateral direction using proton beam micromachining. Firstly, the spread of the protons from the ideal straight path as they interact with the resist material, and secondly, the spatial energy deposition around the proton track due to δ-ray energy deposition.

Monte Carlo calculations were performed to generate the proton trajectories using the computer code TRIM [6]. Two different incident proton energies of 2.0 and 3.5 MeV were used in a calculation of 10^5 proton trajectories in PMMA (density of 1.19 g/cm^3). The distance of the protons from the ideal straight path was determined for different planes at well defined depths from the surface of the resist. The proton positions in the planes at a distance of 5 μm down to 48 μm from the surface for both 2.0 and 3.5 MeV protons were calculated. In addition, for 3.5 MeV protons, which have a 2.6 times larger penetration depth, the spread at the planes located 75, 100, 125 and 150 μm from the surface was also calculated.

To determine the spatial energy deposition around the proton track, we employed a model that describes the radial distribution of dose around the path of an ion [7,8]

$$D(r) = (K(r) + 1)$$
$$\times \frac{Ne^4 Z^{*2}}{\alpha m v^2 r} \left[\frac{(1 - (r + \theta/R + \theta))^{1/\alpha}}{r + \theta} \right]. \quad (1)$$

Here Z^* is the effective charge given by [9], the ion velocity v through the resist containing N electrons per cm^3. The electron charge and mass are given by e and m, respectively. R is the maximum range of the δ-rays, r the distance from the ion track and θ is the range of an electron with specific energy. In our case the constant $\alpha = 1.667$. Finally $K(r)$ is a correction to account for the radial dose due to primary events in the region of $r = 1$–10 nm [8].

The shape of the δ-ray excitation is determined according to Eq. (1) for selected proton energies, which correspond to the average proton energies after penetrating the resist material down to the pre-determined planes. The total energy distribution in the selected planes was then determined by convolution of the δ-ray excitation and the proton distribution.

3. Results

Fig. 1 shows proton micromachined thin walls supported by buttress walls produced in bulk PMMA. The PMMA was exposed using a 2.0 MeV proton beam with a dose of 80 nC/mm^2. The sample was subsequently developed as described in [10]. It is readily noticed that the thin walls have been undercut by the lateral spread of the proton beam. Note that PMMA is a positive resist i.e. exposed regions are removed by the developer. The details of the interaction of the ion beam with the resist material, e.g. the dependence of the threshold dose on the beam energy at a given depth, are currently under investigation.

The detrimental effect of the beam energy spread can be avoided in thin resist films, as demonstrated in Fig. 2. A thin (36 μm) layer of SU-8 negative resist has been applied on a Si wafer
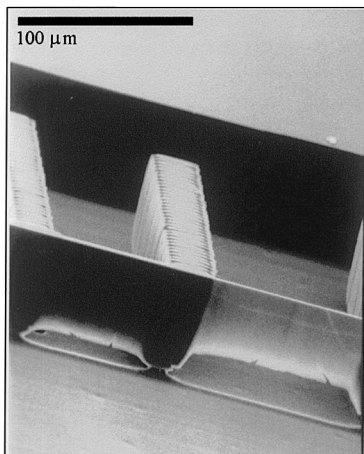
Fig. 1. SEM micrograph showing thin walls supported by thick buttress walls produced in thick PMMA using 2.0 MeV protons.

substrate. The SU-8 was exposed with a 2.0 MeV proton beam (dose 30 nC/mm^2, see Fig. 2(a)), which has a penetration depth in SU-8 of about 60 μm (i.e. the beam passes through the SU-8 resist and stops in the substrate). The sample was subsequently developed as described in [5]. In Fig. 2(b) the same structure was exposed using the proton energy of 1.0 MeV (dose 10 nC/mm^2). Since the protons have a range of about 20 μm in SU-8, the protons will stop in the resist. Since SU-8 is a

negative resist only the exposed resist will remain after development. The exposed structure is then not directly connected to the Si substrate, to prevent the structure from being detached from the Si wafer a support in the centre was made using 2.0 MeV protons (dose 30 nC/mm^2). From the profile of the side walls in Fig. 2(b) it is clear that the end of range ion spread in the 1.0 MeV case causes the structure to widen. On the other hand the walls are relatively straight in the 2.0 MeV exposure because the end of range beam spread occurs in the Si substrate. The experimental results tend to suggest that, at least at the end of range, the dose distribution is determined primarily by the proton beam end of range broadening.

In Fig. 3 the results of the convolution calculations are presented for planes at depths of 5 μm down to 30 μm from the surface, in 5 μm increments. Fig. 3 represents calculations for 2.0 MeV protons and 3.5 MeV protons incident on PMMA. The inset in Fig. 3(a) shows a cut though the convoluted distribution in a plane 20 μm below the surface for 2.0 MeV protons. In this inset, the y-axis represents the energy deposition per nm^3. The integral of the convoluted distribution (19.6 eV/nm) matches closely to the stopping power (23.1 eV/nm) of a proton beam with an energy of 1.578 MeV, representing the average energy of the protons at a depth of 20 μm. The widths of the
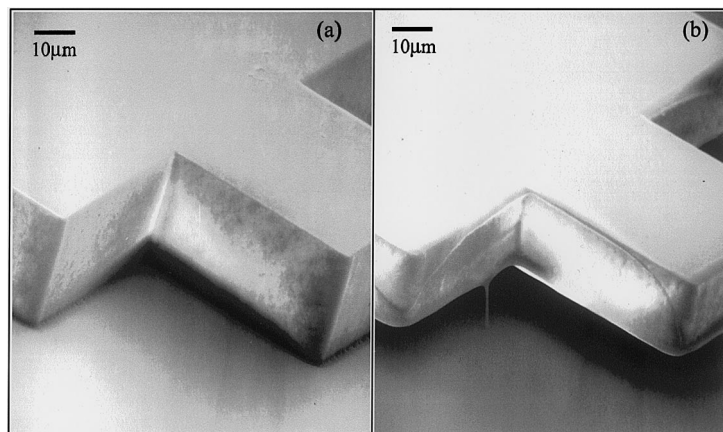
Fig. 2. SEM micrograph of crosses produced in one single layer of 36 μm thick SU-8 using (a) 2.0 MeV protons and (b) 1.0 and 2.0 MeV protons.
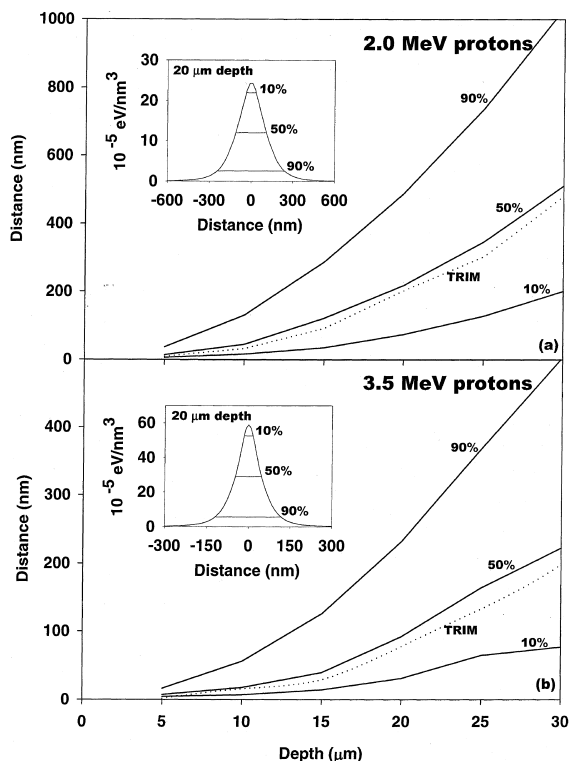
Fig. 3. Results of the convolution calculations as a function of depth for (a) 2.0 MeV protons and (b) 3.5 MeV protons. Insets show the energy deposition at a depth of 20 μm.

Fig. 4. Radial energy deposition as a function of depth for 2.0 MeV protons in PMMA.

distribution at 10%, 50% (FWHM) and 90% of the maximum energy deposition are plotted as chosen representative values of the dose required to expose the resist, since in general resist materials have different sensitivities to energy deposition. These figures of merit were calculated for each of the depth planes and are plotted in Fig. 3. To show the relative effect of the broadening due to δ-rays, the FWHM for the primary proton distribution (using TRIM) is displayed (dotted line) for comparison. These results are in agreement with earlier preliminary calculations [5,10,11].

For both energies the effect of the increase in width due to the δ-rays is less than 32 nm at the FWHM. Beyond a depth of 35 μm, where the proton beam broadening is becoming increasingly significant, there is little difference between the pure TRIM data and the convoluted data. At a depth of 100 μm the FWHM for the 3.5 MeV

proton beam has increased to 2.0 μm and reaches 3.8 μm at a depth of 150 μm.

In Fig. 4, a 3D representation of the radial energy deposition perpendicular to the ion path is plotted versus distance from the surface for 2.0 MeV protons. As can be seen, within the first 10 μm depth, the great majority of the energy deposition is confined well within 100 nm.

4. Conclusions

From the convolution calculations it is clear that beyond a depth of about 35 μm, the lateral broadening of the proton beam is significantly greater than the effects due to δ-ray energy deposition. The effects of δ-ray production on the increase of the spatial energy deposition around an ion track is limited to a maximum of 32 nm at a typical depth of 20 μm for 2.0 and 3.5 MeV protons in PMMA. For penetration depths of about 20 μm therefore the total beam energy deposition is very well confined. As an example, the width of the deposited energy distribution at 50% of the maximum energy deposition is confined within 100 nm of the straight beam path down to a depth of 21 μm for 3.5 MeV protons. For 2.0 MeV

protons the beam is confined within 100 nm down to a depth of 13 μm. This suggests that there are no physical constraints in the future production of high-aspect ratio, sub-100 nm structures.

References

[1] H. Lorenz et al., Proceedings of MME'96 (Micro Mechanics Europe), Barcelona, Spain, October 1996.

[2] T. Osipowicz, J.A. van Kan, T.C. Sum, J.L. Sanchez, F. Watt, Nucl. Instr. and Meth. 161–163 (2000) 83.

[3] J.A. van Kan, J.L. Sanchez, T. Osipowicz, F. Watt, microsystem technologies, accepted (HARMST conference '99).

[4] J.A. van Kan, J.L. Sanchez, B. Xu, T. Osipowicz, F. Watt, Nucl. Instr. and Meth. B 158 (1–4) (1999) 179.

[5] J.A. van Kan, J.L. Sanchez, B. Xu, T. Osipowicz, F. Watt, Nucl. Instr. and Meth. B 148 (1999) 1085.

[6] J. Biersack, L.G. Haggmark, Nucl. Instr. and Meth. 174 (1980) 257.

[7] Zhang Chunxiang, D.E. Dunn, R. Katz, Radiat. Protect. Dos. 13 (1985) 215.

[8] M.P.R. Waligorski, R.N. Hamm, R. Katz, Nucl. Tracks Radiat. Meas. 11 (6) (1986) 309.

[9] W.H. Barakas, Nuclear Research Emulsions, vol. 1, Academia Press, New York, 1963, p. 371.

[10] S.V. Springham, T. Osipowicz, J.L. Sanchez, L.H. Gan, F. Watt, Nucl. Instr. and Meth. B 130 (1997) 155.

[11] S.V. Springham, T. Osipowicz, J.L. Sanchez, S. Lee, F. Watt, SPIE 3183 (1997) 128.